








Cite this: *Nanoscale*, 2024, **16**, 2444

# Minimal numerical ingredients describe chemical microswimmers' 3-D motion†

Maximilian R. Bailey, <sup>a,b</sup> C. Miguel Barriuso Gutiérrez, <sup>b</sup> José Martín-Roca,<sup>b,c</sup> Vincent Niggel,<sup>a</sup> Virginia Carrasco-Fadanelli,<sup>d</sup> Ivo Buttinoni, <sup>d</sup> Ignacio Pagonabarraga, <sup>e,f</sup> Lucio Isa <sup>a</sup> and Chantal Valeriani <sup>\*b,g</sup>

The underlying mechanisms and physics of catalytic Janus microswimmers is highly complex, requiring details of the associated phoretic fields and the physiochemical properties of catalyst, particle, boundaries, and the fuel used. Therefore, developing a minimal (and more general) model capable of capturing the overall dynamics of these autonomous particles is highly desirable. In the presented work, we demonstrate that a coarse-grained dissipative particle-hydrodynamics model is capable of describing the behaviour of various chemical microswimmer systems. Specifically, we show how a competing balance between hydrodynamic interactions experienced by a squirmer in the presence of a substrate, gravity, and mass and shape asymmetries can reproduce a range of dynamics seen in different experimental systems. We hope that our general model will inspire further synthetic work where various modes of swimmer motion can be encoded *via* shape and mass during fabrication, helping to realise the still outstanding goal of microswimmers capable of complex 3-D behaviour.

Received 27th July 2023,  
Accepted 13th December 2023

DOI: 10.1039/d3nr03695b

rsc.li/nanoscale

## 1. Introduction

In the last two decades, potential applications for directed transport at length scales where thermal fluctuations are important have prompted the development of a range of synthetic microswimmers, each with its intricacies.<sup>1–3</sup> Amongst the various synthetic active materials, Janus catalytic microswimmers remain one of the most popular due to their straightforward fabrication protocols, simple experimental setups, and good reproducibility between experiments.<sup>4,5</sup> Typically, these are spherical particles asymmetrically modified with a catalytic material leading to the production of asymmetric local chemical gradients in the presence of a

“fuel”, causing propulsion *via* self-phoresis.<sup>6–9</sup> Such microswimmers generally move in 2-D (*xy*) due to their density mismatch with the surrounding fluid and attractive interactions with the underlying substrate.<sup>10</sup> However, controlling the motion of microswimmers in 3-D is appealing from an applications perspective, and there is a growing body of work on active materials capable of motion in all dimensions.<sup>11–22</sup>

The rational design of chemical microswimmers displaying tailored motion in 3-D would greatly profit from models which can capture empirical observations.<sup>16</sup> However, their experimental simplicity masks a complex system of chemical and mass transfer relationships, the underlying mechanisms and physics of which are still the subject of ongoing debate.<sup>23,24</sup> It is generally accepted that a more complete description of such “chemically active colloids” requires the full solution of their phoretic fields, including details of the colloids, the substrate, and the solution composition.<sup>25–27</sup> Unfortunately, such detailed descriptions call for a high level of technical expertise, are system-specific due to phoretic mobility parameters, have only been solved for spherical and ellipsoidal structures, and do not easily allow the inclusion of thermal fluctuations, which are critical when describing the dynamics of micron-scale objects.

To avoid the consideration of chemical phoretic fields and only account for hydrodynamic flows, the “squirmer” model is frequently invoked.<sup>28</sup> This model was first proposed for microorganisms such as *Paramecia* and *Volvox*,<sup>29,30</sup> and is now used as a generic description for various active systems. Squirmer

<sup>a</sup>Laboratory for Soft Materials and Interfaces, Department of Materials, ETH Zürich, Zürich, Switzerland

<sup>b</sup>Departamento de Estructura de la Materia, Física Térmica y Electrónica, Universidad Complutense de Madrid, Madrid, Spain. E-mail: cvaleriani@ucm.es

<sup>c</sup>Departamento de Química Física, Facultad de Química, Universidad Complutense de Madrid, Madrid, Spain

<sup>d</sup>Department of Physics, Institute of Experimental Colloidal Physics, Heinrich-Heine University, Düsseldorf, Germany

<sup>e</sup>Departament de Física de la Matèria Condensada, Universitat de Barcelona, Barcelona, Spain

<sup>f</sup>Universitat de Barcelona Institute of Complex Systems (UBICS), Universitat de Barcelona, Barcelona, Spain

<sup>g</sup>GISC - Grupo Interdisciplinar de Sistemas Complejos, Madrid, Spain

†Electronic supplementary information (ESI) available: Further details of numerical results and extracted parameters. See DOI: <https://doi.org/10.1039/d3nr03695b>



swim due to a self-generated, usually stationary<sup>31</sup> and axi-symmetric velocity field which is typically evaluated as tangential across its surface. Considered as a spherical rigid body, the squirmer can be defined using two modes describing its swimming velocity and force-dipole ( $B_1$  and  $B_2$  respectively<sup>32</sup>). Promisingly, it has been shown that a bottom-up model of Janus self-diffusiophoretic microswimmers – accounting for the unique interaction potentials of the different chemical species with the separate hemispheres of a Janus particle – will produce flow fields characteristic of spherical squirmers.<sup>33</sup> Recent experimental studies investigating tracer flows around chemical microswimmers<sup>34</sup> and their directed motion under flow (“rheotaxis”)<sup>35,36</sup> have also indicated that the flow fields generated by such active agents are characteristic of squirmer-type systems. Therefore, “coarse-graining” Janus chemical microswimmers as squirmers provides a viable approach to model their behaviour despite neglecting the (albeit important) contributions arising from chemical fields<sup>26,27</sup> and an asymmetric surface.<sup>33</sup>

A number of numerical strategies have been implemented to simulate the coarse-grained dynamics of (chemical) microswimmers, amongst which a multi-particle-collision dynamics (MPCD) description of the solvent is perhaps the most frequently invoked due to its ability to include thermal fluctuations at a lower computational cost than *e.g.* the Lattice Boltzmann (LB) method.<sup>32,37–46</sup> Nevertheless, we note particularly relevant studies where LB approaches were utilised to study the behaviour of raspberry-type and other shape anisotropic microswimmers.<sup>47,48</sup> Like MPCD, dissipative particle dynamics (DPD)<sup>49</sup> coarse-grains the solvent as point-like fluid particles (packets of fluid molecules), and thus inherently includes the effects of thermal noise while solving the Navier-Stokes equations.<sup>50</sup> By utilising a particle-based approach to model the solvent, the computational cost is significantly reduced, allowing the simulation of hydrodynamic interactions in systems where advection dominates over diffusion (high Péclet number,  $Pe$ ).<sup>51</sup> In DPD, the solvent particles themselves act as local thermostats due to their competing stochastic and dissipative pair-wise terms, conserving momentum and thus accounting for hydrodynamics and thermal fluctuations.<sup>52</sup> Additionally, DPD makes use of softer inter-particle potentials, allowing greater timesteps compared to MPCD, thereby enabling simulations of larger systems at longer timescales.<sup>53,54</sup> Therefore, DPD emerges as a suitable candidate to model microswimmers as squirmers, as it can handle hydrodynamics in high  $Pe$  systems (where directed motion dominates over diffusion) with (relatively) large time-steps, while properly dealing with thermal fluctuations. For these reasons, a DPD framework capturing the hydrodynamic interactions of microswimmers in the presence of confining boundaries – by applying tangential solvent forces around the swimmer – was recently developed by some of the authors.<sup>55</sup> As DPD is already implemented in the open-access molecular dynamics program Large-scale Atomic/Molecular Massively Parallel Simulator (LAMMPS),<sup>56</sup> this provides the opportunity to exploit a range of in-built functions to extend previous

studies, with the goal of mimicking the behaviour of chemical microswimmers above a substrate.

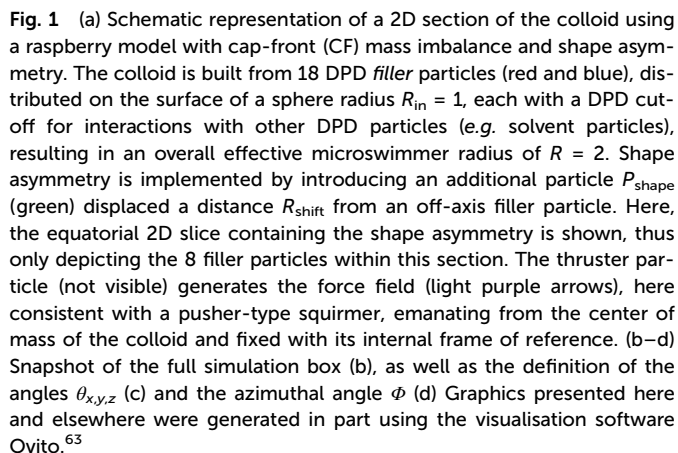
Here, we further develop this model to consider the influence of mass and shape asymmetries on the dynamics of spherical microswimmers in the presence of a bounding substrate, mirroring common experimental conditions for chemical active colloids.<sup>55,57–59</sup> The strength of our approach lies in its modularity, which allows the simple inclusion of these asymmetries that may have otherwise presented significant complications when considering other numerical schemes. We find that the interplay between hydrodynamic interactions, gravity, bottom-heaviness, and shape is sufficient to qualitatively capture the 2- and 3-D physics of a range of catalytic (and photo-catalytic) Janus microswimmer systems,<sup>17,18,20</sup> *i.e.* while neglecting contributions from chemical<sup>59</sup> and light<sup>60,61</sup> gradients. Specifically, there is a competition between the hydrodynamic attraction to the substrate that grows with the swimming speed and the active force required to overcome gravity, which determines the ability of the microswimmer to enter the bulk. This balance can be furthermore adjusted by introducing mass or shape asymmetry to the particles. Our coarse-grained approach thus opens the door to the informed design of chemical microswimmers whose dynamics can be encoded *via* shape or mass during fabrication, helping to realise the still outstanding goal of active colloids capable of truly 3-D dynamics.

## 2. Numerical method

Following the approach outlined in ref. 55, we use an in-house extension of the open source LAMMPS package<sup>56</sup> to simulate the motion of squirmer-like microswimmers, modelled as rigid-body raspberry structures constructed from DPD “filler” spheres using the LAMMPS fix-rigid module (see Fig. 1). The thermal energy of the solvent particles  $k_B T$  is set to 1, the solvent density  $\rho = 5.9$  (where  $\rho = N_p V_p / V_{\text{system}}$ , for  $N_p$  solvent particles with volume  $V_p$ , in a simulation volume  $V_{\text{system}}$ ), and the dissipative force  $\gamma = 1$ . The simulation length-scales are as described in Fig. 1a, normalised with respect to the radius of 1 DPD filler particle, while the masses of DPD particles are set to 1 unless introducing mass asymmetry (see below). Solvent DPD spheres (purple particles, see Fig. 1) interact with the microswimmer’s constituent “filler” particles with a DPD cutoff of  $R_{fs} = 2$  while between them we set  $R_{ss} = 0.58$  to achieve a lower Reynolds number.<sup>49</sup> The simulation time-scale  $\tau$  is set according to these parameters, and numerically integrated at  $0.01\tau$  time-steps. When present, substrates are modelled as overlapping DPD particles (see Fig. 1b (ref. 55)), properly aligned along the  $x$ - and  $y$ -axes to ensure a flat repulsive potential interacting with both the solvent and colloid particles *via* the DPD soft conservative force with a large amplitude  $F_c = 100$ .<sup>49</sup>

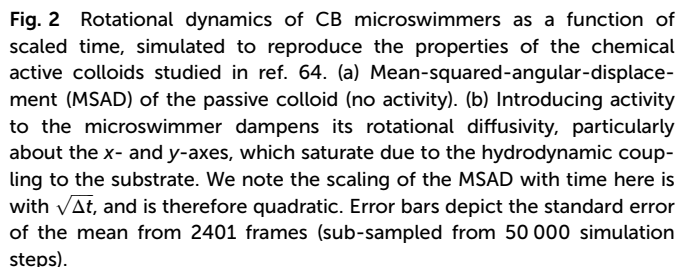
The microswimmers motility originates from one central “thruster” particle, which generates the squirmer-type force field experienced by the solvent particles in the spherical shell between the outer surface of the microswimmer (dashed black




$$m_{\text{asymm}} = \frac{m_{\text{hemisphere}} + m_{\text{cap}}}{m_{\text{hemisphere}}}$$

### 3. Results & discussion

To begin, we consider colloids characterised by hydrodynamic interactions with a surface and bottom-heaviness, and study their dynamics with or without activity. Specifically, we reproduce the ‘classic’ Pt-SiO<sub>2</sub> Janus chemical microswimmers to determine whether our DPD raspberry particle model captures their dynamics. We investigate the chemical microswimmers studied by Niggel *et al.*,<sup>64</sup> as the 3-D rotations of the Janus particles with fluorescent surface asperities can be tracked *via* correlation-based image analysis. To reproduce their experimental findings, we simulate the microswimmers with CB motion and  $m_{\text{asym}} = 1.081$ . Fitting the short-time mean-square-displacement (MSD) of those chemical microswimmers ( $\text{MSD} = 4D_{\text{T}}\Delta t + v_{\text{p}}^2\Delta t^2$ , while acknowledging its shortcomings<sup>65</sup>), we obtain a Péclet number  $\text{Pe} = \frac{v_{\text{p}} \cdot R}{D_{\text{T}}} \sim 300$  (where  $v_{\text{p}}$ ,  $D_{\text{T}}$  are the fitted swimming speed and translational diffusion coefficient from the MSD, respectively, and  $R$  is the particle radius), which we set to  $\sim 100$  in simulations of our active microswimmers to ensure that they remain in the low Reynolds regime as described above. Likewise, we set the gravitational force such that  $V_{\text{gravity}} \sim V_{\text{swim}}$ , for  $V_{\text{swim}} = \langle v_0 \rangle$ , where  $v_0$  is the microswimmer’s instantaneous velocity over time. As we have access to the structural coordinates of our DPD raspberries, we are able to follow their rotational dynamics *via* singular value decomposition (SVD) and calculate the cumulative mean-squared-angular-displacement (MSAD) (see Fig. 2 (ref. 66)). By doing so, we are able to reproduce the findings presented in.<sup>64</sup> Specifically, we find that for passive particles, the presence of a heavy cap and a substrate reduces the rotation “out-of-plane” ( $\theta_{x,y}$ ) compared to in plane ( $\theta_z$ ) rotations (see Fig. 1c and d) due to bottom-heaviness (see Fig. 2a (ref. 67)), while the introduction of activity saturates the out-of-plane rotation at much lower values (Fig. 2b). We attribute the confinement of possible rotations to the hydrodynamic attraction between the microswimmer and the substrate due to its generated flow fields,<sup>68</sup> mirrored by later theoretical investigations into the role of the produced phoretic fields.<sup>10</sup> Therefore, we see that the rotational dynamics of chemical microswimmers near confining boundaries are qualitatively well captured when only considering hydrodynamic interactions (and bottom-heaviness).

[illegible]

**Fig. 3** Dynamics of CB microswimmers, simulated to reproduce the properties of the chemical active colloids studied in.<sup>20</sup>  $z/R$  refers to the height that a microswimmer reaches above the substrate with respect to its radius  $R$  (a, d, and g).  $\Phi$  is the azimuthal angle of the microswimmer (b, e, and h) as defined in Fig. 1, and  $v_0$  is the time-series of the microswimmer's instantaneous velocity (c, f, and i, with  $V_{\text{swim}} = \langle v_0 \rangle / R$ ). The insets in (a) and (g) show the solvent velocity flow fields around the (fixed) microswimmer at the different self-propulsion forces. Here, we progressively increase the swimming to sedimentation velocity ( $V_{\text{swim}} : V_{\text{gravity}}$ ) from top to bottom to qualitatively map onto the different systems studied by Carrasco-Fadanelli and Buttinoni. The first two cases (a–c and d–f) are in good agreement with the findings presented in ref. 20, while the final case (g–i) recaptures the typical dynamics observed for chemical active colloids, where phoretic particles are essentially confined to 2-D (also see Fig. 2b).

To summarise, we find that hydrodynamic interactions and gravitational forces on a mass-asymmetric spherical microswimmer are sufficient to qualitatively capture the physics of chemical microswimmers above a substrate under different conditions. We also confirm the importance of gravity on both the translational and rotational dynamics of active colloids suspended just above a planar surface.

Motivated by the ability of the reported DPD squirmer-like microswimmers to qualitatively reproduce the behaviour of different chemical microswimmers, we then investigate strategies to promote the “lift-off” of particles from the substrate, and thus observe 3-D motion. Recently, photocatalytic microswimmers synthesised using functional nanoparticles *via* “Toposelective Nanoparticle Attachment” were shown to display quasi 3-D behaviour,<sup>17–19</sup> characterised by 2-D motio-

ninterdispersed with “rollercoaster”-like looping behaviour. This happens in spite of their high speeds with respect to their sedimentation speed, putting them in a regime closer to the third case highlighted in Fig. 3(g–i), as well as their CF motion which should in fact promote orientation into the wall due to top-heaviness. We note the use of surface-bound functional nanoparticles incorporates rough asperities to the microswimmers, which in turn introduce asymmetry in the drag acting on the surface of the microswimmers. In fact, explicitly considering non-axisymmetric flow fields in spherical squirmers was very recently shown to induce body rotations and thus complex patterns of motion.<sup>69</sup> To investigate the potential effect of such shape-asymmetries on the motion of microswimmers, we simulate the motion of our DPD raspberries with introduced shape asymmetry in the absence of gravity or bounding substrates, this time with CF swimming (see Fig. 4). Specifically, we introduce weightless “shape” particles ( $P_{\text{shape}}$ ) along the axis of the existing “filler” particles, shifted by different distances (normalised by the DPD particle radius –  $R_{\text{shift}}$ ) to control the extent of its protrusion (see Fig. 1a). The filler particle axis along which the shape particle is introduced can be changed to modify the extent of asymmetry, *i.e.* with respect to the swimming direction (see ESI S5†). We focus on the case where  $P_{\text{shape}}$  is introduced so as to maximise the shape-asymmetry possible using this approach (see Fig. 1a, ESI Fig. S5,† “1 Edge” case).

To quantify the effect that increasing  $R_{\text{shift}}$  has on the dynamics of our bulk microswimmers, we calculate the angle,  $\theta$ , between the vectors describing the particle's internal orientation axis,  $\mathbf{A}$ , (governing the direction of the self-propulsion

force, see Fig. 1a), and the particles displacement vector,  $\mathbf{B}$ , ( $\theta = \arccos\left(\frac{\mathbf{A} \cdot \mathbf{B}}{|\mathbf{A}||\mathbf{B}|}\right)$ ), where  $\mathbf{A}$  is defined by 3 particles along the microswimmers body axis at time  $t$  and  $\mathbf{B} = [x_{t+\Delta t} - x_t, y_{t+\Delta t} - y_t, z_{t+\Delta t} - z_t]$ . We note that the value of  $\langle\theta\rangle$  is dependent on the  $\Delta t$  over which the displacement vector is evaluated. We find a positive correlation between  $R_{\text{shift}}$  and  $\langle\theta\rangle$  (coefficient of determination = 0.953, see Fig. 4a), which we attribute to the increasing torque experienced by the microswimmer due to the solvent forces applied to  $R_{\text{shape}}$  at the distance  $R_{\text{shift}}$ . We hypothesise that the non-zero value for  $\langle\theta\rangle$  at  $R_{\text{shift}} = 0$  arises due to the presence of thermal fluctuations from the solvent and their effect on microswimmer motion (see ESI, Fig. S4† for further discussion). The source of the growing divergence between the internal orientation of the particles and their swimming velocity can also be observed in the MSAD of the microswimmers as the trends become increasingly ballistic with larger  $R_{\text{shift}}$  (see ESI, Fig. S6†). Notably, the fitted angular velocity  $\omega$  (ballistic component of the MSAD,  $\text{MSAD} = 2D_R\Delta t + \omega^2\Delta t^2$ , where  $D_R$  is the rotational diffusion coefficient) grows with shape asymmetry, and we determine a strong linear relationship between  $\omega$  and  $\langle\theta\rangle$  (see Fig. 4a, bottom inset – coefficient of determination = 0.981). We furthermore note a linear growth of the “rotational” Péclet ( $\text{Pe}_R = \frac{\omega \cdot \Delta t}{\sqrt{D_R \cdot \Delta t}}$ ) with  $R_{\text{shift}}$  (see Fig. 4b, coefficient of determination = 0.982), demonstrating the increasingly deterministic orientational motion of the microswimmer as shape asymmetry becomes more pronounced. Finally, we note that introducing  $P_{\text{shape}}$  along axes resulting in a reduced shape asymmetry with respect to  $\mathbf{A}$  have a negligible effect on  $\theta$ , indicating the importance of appropriate shape selection (see ESI; Fig. S5, S7, and S8†).

After establishing the effect of shape asymmetry on microswimmer motion in the absence of external fields and confining boundaries, we then introduce gravity and a substrate to simulate the experimental conditions in ref. 17 and 18 using  $m_{\text{asym}} = 1.25$ . We define  $V_{\text{swim}} : V_{\text{sediment}} \sim 1.5$  to prevent the microswimmers from escaping too far into the bulk. Under these conditions, microswimmers with no or low shape asymmetry are unable to leave the bottom substrate due to the joint forces of gravity and hydrodynamic attraction (see Fig. 5a). However, beyond a threshold value of  $R_{\text{shift}} > 0.25$ , the microswimmers display 3-D motion and begin to loop into the bulk, demonstrated by the emerging tail in  $P(z/R)$ . This ability to leave the substrate is reflected in the angles which the internal orientation of the microswimmer makes with the substrate,  $\Phi$ . Specifically, with increasing shape asymmetry, we observe an increase in positive values in the distribution  $P(\Phi)$  (see Fig. 5b), which indicates that the particle points upwards and away into the bulk, thus overcoming gravity.

We thus propose that the angular velocity  $\omega$ , introduced by the shape asymmetry of the microswimmers, drives its internal swimming orientation away from the substrate, competing with the effects of gravity and hydrodynamic wall interactions (as well as thermal fluctuations). Above a certain threshold

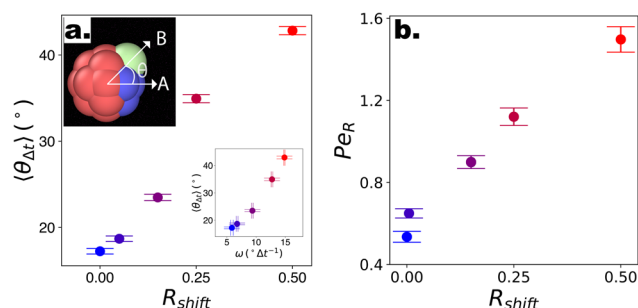


**Fig. 4** Swimming dynamics of CF microswimmers with respect to their cap orientation, in the absence gravity and bounding substrates, as a function of introduced shape asymmetry  $R_{\text{shift}}$  (colour coded from blue to red with increasing  $R_{\text{shift}}$ ). (a) Increasing divergence  $\langle\theta\rangle$  in the internal body axis and the observed swimming direction is measured with increasing  $R_{\text{shift}}$ . We note that the values of  $\langle\theta\rangle$  are a function of the time-step evaluated (here,  $\sqrt{D_T\Delta t}/R \sim 0.13$ , where  $D_T$  is the constant obtained for a passive sphere with  $R_{\text{shift}} = 0$ ). Inset: linear growth in  $\langle\theta\rangle$  with  $\omega$  values fitted from the microswimmers' MSAD (see ESI, Fig. S6†). Graphical inset: angle  $\theta$  between the swimming direction and internal body axis, as defined in the text. The particle depicted has  $R_{\text{shift}} = 0.5$ . (b) Rotational Péclet number as a function of  $R_{\text{shift}}$  for  $\Delta t = 1$ . Error bars either indicate the standard error of the mean, or for the fits of  $\omega$  and  $D_R$  are obtained from the co-variance matrix, accounting for error propagation where relevant, from 1001 frames (sub-sampled from 50 000 simulation steps).



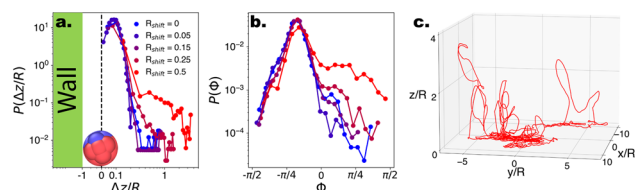


**Fig. 5** Probability distributions for CF microswimmers describing their out-of-plane motion  $P(\Delta z/R)$  and orientation  $P(\phi)$ , as a function of their introduced shape asymmetry  $R_{\text{shift}}$  indicated by the colour code in the legend. (a) Above a threshold ( $R_{\text{shift}} > 0.25$ ), the microswimmers are able to leave the substrate and enter the bulk. For visualisation,  $\Delta z$  where  $\Delta z/R < 0.05$  is set to 0, and the presence of the wall is indicated. The particle depicted at the wall has an orientation  $\phi \sim -\pi/8$ . (b) The ability to leave the substrate is reflected in the emergence of a shoulder in  $P(\phi)$  for  $\phi > 0$ , as  $V_{\text{swim}} > V_{\text{gravity}}$  and therefore the microswimmer can overcome its sedimentation velocity and enter the bulk. (c) Example quasi-3D trajectory of a microswimmer with  $R_{\text{shift}} = 0.5$ . Note that the motion is predominantly in the xy plane, with looping out-of-plane (z) segments as described in ref. 17–19.

shape asymmetry – governed by the dynamics of the system – the microswimmer is able to escape the substrate and move out-of-plane.

In summary, we demonstrated that shape asymmetry is an important design parameter to control the dynamics of chemical microswimmers, in particular to promote 3-D motion. Specifically, the presence of these introduced asperities explains the unconventional swimming patterns observed in some experimental systems.<sup>17,18</sup>

## 4. Conclusions

By extending the DPD numerical framework described in<sup>55</sup> to include the effects of mass and shape asymmetries, we have demonstrated that hydrodynamic interactions, gravity, and thermal fluctuations are sufficient to capture the dynamics of a range of experimental chemically active colloidal systems.<sup>17,18,20,64</sup> Promisingly, the use of DPD particles to build the overall structure of the microswimmer enables us to access to a range of more complex shapes than those described here, whose formulation would otherwise be either intractable or highly challenging when using other numerical modelling frameworks, or explicitly including chemical fields. We believe that our numerical simulations could be used in the design of new chemical colloidal swimmers, *e.g.* via sequential-capillarity-particle-assembly (sCAPA)<sup>70</sup> or two-photon polymerization direct laser writing (2PP-DLW),<sup>71</sup> with the goal of realising chemical microswimmers capable of 3-D motion. Furthermore, this modular approach to generating complex structures enables the study of microswimmer physics considering arbitrary geometries, *e.g.* swimming above rough surfaces<sup>20</sup> or along inclined walls,<sup>22</sup> informing experiments into the interactions of active materials with confining boundaries commonplace in applied settings. To conclude, we foresee DPD based approaches to microswimmer modelling to provide

opportunities in the development and application of chemically active colloids.

## Author contributions

Author contributions are defined based on the CRediT (contributor roles taxonomy). Conceptualization: M. R. B., C. M. B. G., L. I., C. V. Discussions: M. R. B., C. M. B. G., J. M. R., V. N., V. C., I. B., I. P., L. I., C. V. Formal analysis: M. R. B., C. M. B. G. Funding acquisition: M. R. B., L. I. Investigation: M. R. B. Methodology: M. R. B., C. M. B. G., J. M. R. Software: M. R. B., C. M. B. G., J. M. R. Supervision: L. I., C. V. Validation: M. R. B. Visualization: M. R. B., C. M. B. G., L. I. Writing – original draft: M. R. B., C. M. B. G., L. I. Writing – review and editing: M. R. B., C. M. B. G., J. M. R., V. N., I. B., I. P., L. I., C. V.

## Conflicts of interest

There are no conflicts to declare.

## Acknowledgements

M. R. B. acknowledges financial support from the ETH Zurich Doc.Mobility Fellowship scheme. I. P. acknowledges support from Ministerio de Ciencia MCIN/AEI/FEDER for financial support under grant agreement PID2021-126570NB-I00 AEI/FEDER-EU, and from Generalitat de Catalunya under Program Icrea Academia and project 2021SGR-673. C. V. acknowledges financial support from MINECO under grant agreements EUR2021-122001, PID2019-105343GB-I00, IHRC22/00002, and PID2022-140407NB-C21.

## References

- 1 S. Ramaswamy, *Annu. Rev. Condens. Matter Phys.*, 2010, **1**, 323–345.
- 2 C. Bechinger, R. Di Leonardo, H. Löwen, C. Reichhardt, G. Volpe and G. Volpe, *Rev. Mod. Phys.*, 2016, **88**, 045006.
- 3 G. Gompper, R. G. Winkler, T. Speck, A. Solon, C. Nardini, F. Peruani, H. Löwen, R. Golestanian, U. B. Kaupp, L. Alvarez, *et al.*, *J. Phys.: Condens. Matter*, 2020, **32**, 193001.
- 4 J. R. Howse, R. A. Jones, A. J. Ryan, T. Gough, R. Vafabakhsh and R. Golestanian, *Phys. Rev. Lett.*, 2007, **99**, 8–11.
- 5 W. Wang, X. Lv, J. L. Moran, S. Duan and C. Zhou, *Soft Matter*, 2020, **16**, 3846–3868.
- 6 R. Golestanian, T. B. Liverpool and A. Ajdari, *Phys. Rev. Lett.*, 2005, **94**, 1–4.
- 7 M. N. Popescu, S. Dietrich, M. Tasinkevych and J. Ralston, *Eur. Phys. J. E: Soft Matter Biol. Phys.*, 2010, **31**, 351–367.
- 8 K. K. Dey, F. Wong, A. Altemose and A. Sen, *Curr. Opin. Colloid Interface Sci.*, 2016, **21**, 4–13.



- 9 M. R. Bailey, N. Reichholf, A. Flechsig, F. Grillo and L. Isa, *Part. Part. Syst. Charact.*, 2022, **39**, 2100200.
- 10 W. E. Uspal, M. N. Popescu, S. Dietrich and M. Tasinkevych, *Soft Matter*, 2015, **11**, 434–438.
- 11 A. I. Campbell and S. J. Ebbens, *Langmuir*, 2013, **29**, 14066–14073.
- 12 A. I. Campbell, R. Wittkowski, B. Ten Hagen, H. Löwen and S. J. Ebbens, *J. Chem. Phys.*, 2017, **147**, 084905.
- 13 D. P. Singh, W. E. Uspal, M. N. Popescu, L. G. Wilson and P. Fischer, *Adv. Funct. Mater.*, 2018, **28**, 1706660.
- 14 O. Yasa, P. Erkoc, Y. Alapan and M. Sitti, *Adv. Mater.*, 2018, **30**, 1804130.
- 15 J. G. Lee, A. M. Brooks, W. A. Shelton, K. J. Bishop and B. Bharti, *Nat. Commun.*, 2019, **10**, 2575.
- 16 A. M. Brooks, S. Sabrina and K. J. Bishop, *Proc. Natl. Acad. Sci. U. S. A.*, 2018, **115**, E1090–E1099.
- 17 M. R. Bailey, T. A. Gmür, F. Grillo and L. Isa, *Chem. Mater.*, 2023, **35**, 3731–3741.
- 18 M. R. Bailey, F. Grillo, N. D. Spencer and L. Isa, *Adv. Funct. Mater.*, 2022, **32**, 2109175.
- 19 M. R. Bailey, F. Grillo and L. Isa, *Soft Matter*, 2022, **18**, 7291–7300.
- 20 V. Carrasco-Fadanelli and I. Buttinoni, *Phys. Rev. Res.*, 2023, **5**, L012018.
- 21 O. Chepizhko and T. Franosch, *Phys. Rev. Lett.*, 2022, **129**, 228003.
- 22 Q. Brosseau, F. B. Usabiaga, E. Lushi, Y. Wu, L. Ristroph, M. D. Ward, M. J. Shelley and J. Zhang, *Soft Matter*, 2021, **17**, 6597–6602.
- 23 X. Lyu, X. Liu, C. Zhou, S. Duan, P. Xu, J. Dai, X. Chen, Y. Peng, D. Cui, J. Tang, X. Ma and W. Wang, *J. Am. Chem. Soc.*, 2021, **143**, 12154–12164.
- 24 A. Domínguez and M. N. Popescu, *Curr. Opin. Colloid Interface Sci.*, 2022, **61**, 101610.
- 25 M. N. Popescu, W. E. Uspal, Z. Eskandari, M. Tasinkevych and S. Dietrich, *Eur. Phys. J. E: Soft Matter Biol. Phys.*, 2018, **41**, 1–24.
- 26 J. Katuri, W. E. Uspal, M. N. Popescu and S. Sánchez, *Sci. Adv.*, 2021, **7**, eabd0719.
- 27 J. D. Torrenegra-Rico, A. Arango-Restrepo and J. M. Rubí, *J. Chem. Phys.*, 2022, **157**, 104103.
- 28 A. Zöttl and H. Stark, *Annu. Rev. Condens. Matter Phys.*, 2023, **14**, 109–127.
- 29 M. J. Lighthill, *Commun. Pure Appl. Math.*, 1952, **5**, 109–118.
- 30 J. R. Blake, *Math. Proc. Cambridge Philos. Soc.*, 1971, **70**, 303–310.
- 31 V. Magar, T. J. Pedley and T. Goto, *Q. J. Mech. Appl. Math.*, 2003, **56**, 65–91.
- 32 M. Theers, E. Westphal, G. Gompper and R. G. Winkler, *Soft Matter*, 2016, **12**, 7372–7385.
- 33 M. Yang, A. Wysocki and M. Ripoll, *Soft Matter*, 2014, **10**, 6208–6218.
- 34 A. I. Campbell, S. J. Ebbens, P. Illien and R. Golestanian, *Nat. Commun.*, 2019, **10**, 3952.
- 35 J. Katuri, W. E. Uspal, J. Simmchen, A. Miguel-López and S. Sánchez, *Sci. Adv.*, 2018, **4**, eaao1755.
- 36 P. Sharan, Z. Xiao, V. Mancuso, W. E. Uspal and J. Simmchen, *ACS Nano*, 2022, **16**, 4599–4608.
- 37 A. Malevanets, *J. Chem. Phys.*, 1999, **110**, 8605–8613.
- 38 A. Malevanets and R. Kapral, *J. Chem. Phys.*, 2000, **112**, 7260–7269.
- 39 G. Rückner and R. Kapral, *Phys. Rev. Lett.*, 2007, **98**, 150603.
- 40 S. Thakur and R. Kapral, *Phys. Rev. E: Stat., Nonlinear, Soft Matter Phys.*, 2012, **85**, 026121.
- 41 P. De Buyl and R. Kapral, *Nanoscale*, 2013, **5**, 1337–1344.
- 42 I. Llopis and I. Pagonabarraga, *J. Non-Newtonian Fluid Mech.*, 2010, **165**, 946–952.
- 43 I. Pagonabarraga and I. Llopis, *Soft Matter*, 2013, **9**, 7174.
- 44 F. Alarcon, E. Navarro-Argemí, C. Valeriani and I. Pagonabarraga, *Phys. Rev. E*, 2019, **99**, 062602.
- 45 A. Scagliarini and I. Pagonabarraga, *Soft Matter*, 2022, **18**, 2407–2413.
- 46 A. Zöttl and H. Stark, *Eur. Phys. J. E: Soft Matter Biol. Phys.*, 2018, **41**, 1–11.
- 47 L. P. Fischer, T. Peter, C. Holm and J. de Graaf, *J. Chem. Phys.*, 2015, **143**, 084107.
- 48 J. de Graaf, H. Menke, A. J. Mathijssen, M. Fabritius, C. Holm and T. N. Shendruk, *J. Chem. Phys.*, 2016, **144**, 134106.
- 49 R. D. Groot and P. B. Warren, *J. Chem. Phys.*, 1997, **107**, 4423–4435.
- 50 P. J. Hoogerbrugge and J. M. Koelman, *EPL*, 1992, **19**, 155–160.
- 51 J. M. Koelman and P. J. Hoogerbrugge, *EPL*, 1993, **21**, 363–368.
- 52 P. Espanol and P. Warren, *EPL*, 1995, **30**, 191–196.
- 53 T. Soddemann, B. Dünweg and K. Kremer, *Phys. Rev. E*, 2003, **68**, 046702.
- 54 F. Lugli, E. Brini and F. Zerbetto, *J. Phys. Chem. C*, 2012, **116**, 592–598.
- 55 C. M. Barriuso Gutiérrez, J. Martín-Roca, V. Bianco, I. Pagonabarraga and C. Valeriani, *Front. Phys.*, 2022, **10**, 926609.
- 56 S. Plimpton, *J. Comput. Phys.*, 1995, **117**, 1–19.
- 57 B. ten Hagen, F. Kümmel, R. Wittkowski, D. Takagi, H. Löwen and C. Bechinger, *Nat. Commun.*, 2014, **5**, 4829.
- 58 J. Simmchen, J. Katuri, W. E. Uspal, M. N. Popescu, M. Tasinkevych and S. Sánchez, *Nat. Commun.*, 2016, **7**, 10598.
- 59 S. Das, Z. Jalilvand, M. N. Popescu, W. E. Uspal, S. Dietrich and I. Kretzschmar, *Langmuir*, 2020, **36**, 7133–7147.
- 60 D. P. Singh, W. E. Uspal, M. N. Popescu, L. G. Wilson and P. Fischer, *Adv. Funct. Mater.*, 2018, **28**, 1706660.
- 61 W. E. Uspal, *J. Chem. Phys.*, 2019, **150**, 114903.
- 62 J. T. Padding and A. A. Louis, *Phys. Rev. E: Stat., Nonlinear, Soft Matter Phys.*, 2006, **74**, 1–29.
- 63 A. Stukowski, *Modell. Simul. Mater. Sci. Eng.*, 2010, **18**, 015012.
- 64 V. Niggel, M. R. Bailey, C. van Baalen, N. Zosso and L. Isa, *Soft Matter*, 2023, **19**, 3069–3079.
- 65 M. Bailey, A. Sprenger, F. Grillo, H. Löwen and L. Isa, *Phys. Rev. E*, 2022, **106**, L052602.



- 66 B. Ilhan, J. J. Schoppink, F. Mugele and M. H. Duits, *J. Colloid Interface Sci.*, 2020, **576**, 322–329.
- 67 A. Rashidi, S. Razavi and C. L. Wirth, *Phys. Rev. E*, 2020, **101**, 042606.
- 68 S. E. Spagnolie and E. Lauga, *J. Fluid Mech.*, 2012, **700**, 105–147.
- 69 P. S. Burada, R. Maity and F. Jülicher, *Phys. Rev. E*, 2022, **105**, 1–8.
- 70 S. Ni, E. Marini, I. Buttinoni, H. Wolf and L. Isa, *Soft Matter*, 2017, **13**, 4252–4259.
- 71 R. P. Doherty, T. Varkevisser, M. Teunisse, J. Hoecht, S. Ketzetzi, S. Ouhajji and D. J. Kraft, *Soft Matter*, 2020, **16**, 10463–10469.

